The Evolution of Deep Convection over Africa and the Tropical Atlantic

JM Futyan
Columbia University
New York, New York

AD Del Genio
National Aeronautics and Space Administration
Goddard Institute for Space Studies
New York, New York

Introduction

Deep convection over Africa is among the strongest found anywhere, and its associated cloud and hydrological properties provide an interesting contrast to those associated with the often weakly buoyant convection observed over the Atmospheric Radiation Measurement (ARM) Program tropical warm pool sites. Here, hourly thermal flux data from the geostationary Meteosat-8 satellite are used to identify and track convective cloud systems over the African continent and tropical Atlantic. A multiple threshold 'detect and spread' approach is used to capture all stages of development. The observed system evolution is then used to define the life-cycle stage at each time-step, providing a framework within which other, non-geostationary satellite or in situ data can be used to build up a composite picture of convective system evolution.

The initial analyses presented here used data from instruments on the Tropical Rainfall Measuring Mission (TRMM) satellite to investigate differences in lightning occurrence, rainfall rates, and convective-stratiform partitioning between continental and maritime convective systems as a function of the system development.

This framework will also provide a valuable tool for analysis of data from the African Monsoon Multi-disciplinary Analysis (AMMA) campaign, including data collected by the ARM Mobile Facility during its deployment in Niamey, Niger. We expect the results to provide valuable constraints for the testing of mesoscale updraft and stratiform anvil parameterizations that are currently absent or deficient in GCMs.

Methodology

Detection and Tracking of Convective Systems

Convective systems are identified as continuous regions of cold topped cloud in the broadband thermal flux images from Meteosat-8. As data from the Geostationary Earth Radiation Budget (GERB) experiment are not yet available, GERB-like data, produced using a narrowband to broadband conversion of the Spinning Enhanced Visible and Infra-Red Imager (SEVIRI) data, are used here. To ensure that as much of the cirrus anvil associated with the convective cores as possible is retained, a multiple threshold detect and spread approach, similar to that proposed by Boer and Ramanthan (1997) is used. An initial threshold is applied to the flux image to define cold system cores. These are then grown outwards until either the edge of the system at the second, warmer, threshold value is reached, or until another system is encountered. New systems, without a cold core, are also detected at the new threshold. The process is repeated until all systems have been grown to the warmest threshold value.

By including warmer anvil cloud surrounding cold cores and allowing the system to be tracked through stages of development where no cold core is present, this approach provides a more complete picture of the spatial and temporal structure than tracking with a single threshold. The results presented here are for thresholds at 165, 200, and 235 Wm^{-2} (approximately 232, 244, and 254 K respectively); however, similar results are found for alternative thresholds.

Systems are tracked through their lifecycle using hourly flux data. Tracking is performed iteratively using a maximum area overlap approach. For each system identified in the new image, if the cold core of that system overlaps with more then 50% of the cold core of a system in the previous image they are identified as the same system. If not, or for new systems without cold cores, overlap is calculated at the warmer thresholds. Where two systems merge, the larger, deeper system is considered to continue and the smaller part to terminate. Similarly, where a system splits, the larger fragment is considered as the continuation. All systems present in three or more consecutive images are tracked, but results presented here are only for systems reaching a minimum brightness temperature at some point during their lifetime of less than 220 K and a maximum effective radius of more than 300 km, which we refer to as ”large deep systems.”

Determining Life-Cycle Stage

The evolution of the system radius and minimum brightness temperature is used to define the life-cycle stage. The definition is based on the expected evolution of a convective system, beginning with vertical growth of a cumulus core, followed by detrainment of a cirrus anvil and subsequent dissipation.

For each tracked system, a smooth curve is fitted to the radius and temperature data and used to determine the time where the minimum temperature is reached and the time of maximum spatial extent. Before the minimum in brightness temperature, the system is growing vertically and is considered to be

"developing." The subsequent period of horizontal growth is considered to be the "mature" or "detraining" stage of the system's development, and the system is considered to begin to dissipate after the maximum radius is reached. The developing and dissipating stages are further divided into "cold" and "warm" portions based on the minimum brightness temperature within the cloud. This categorization is illustrated in Figure 1, which shows the temperature and radius data and the resulting life-cycle stage classification for an example African land-based storm.

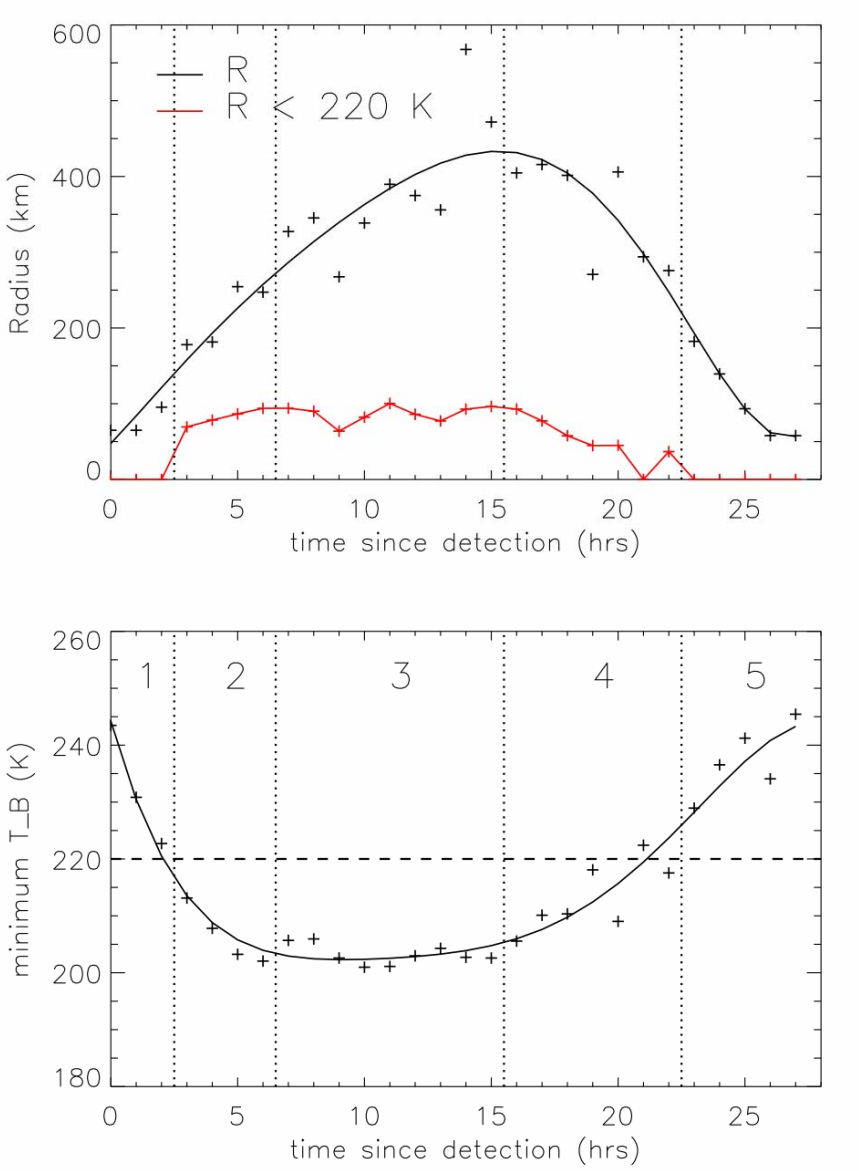

Figure 1. Example of system radius (R) and brightness temperature (T_B) evolution for an African land convective system and the corresponding life-cycle stage classification. Numbers in lower panel give the life-cycle stage: 1. warm developing, 2. cold developing, 3. mature/ detraining, 4. cold dissipating, 5. warm dissipating.

Results

This definition of life-cycle stage provides a framework to compare the evolution of African convective systems with oceanic systems in the Atlantic inter-tropical convergence zone (ITCZ). By matching the tracked systems to over-passes of low earth orbiting satellites such as TRMM or to ground-based data, these less well sampled datasets can also be evaluated as a function of system evolution.

Plotting results as a function of life-cycle stage rather than simply as against time since formation allows data for systems with a wide range of lifetimes to be combined in a meaningful way and allows results for systems where the complete lifecycle is not tracked (for example where the system forms in a split and hence no developing stage is observed) to be included. This approach is particularly valuable for producing composites from relatively sparse datasets.

Observed System Evolution from Geostationary Satellite Data

Figure 2 compares the evolution of the radiative (system averaged outgoing longwave radiation (OLR) and albedo) and precipitation (precipitating area fraction and conditional average rain rate) properties for African land and Atlantic ITCZ systems. Radiative properties are based on hourly GERB-like data and precipitation results are from the three-hourly merged TRMM and geostationary satellites (3B42) dataset for four months (June-September, JJAS) of 2005 for the region 50W-50E, 20S-30N.

Land based systems are deeper and brighter then oceanic systems throughout the life-cycle. However, Atlantic systems show significantly higher precipitating area fractions. The conditional (averaged only over the precipitating portion of the system) rain rates are similar for land and ocean, although oceanic systems remain more heavily precipitating in the dissipating stages. These results are consistent with the presence of larger and more persistent stratiform rain decks over the ocean (Schumacher and Houze 2003).

The lower albedo observed over ocean may, at least in part, be influenced by the lower surface albedo. However, the higher average OLR and minimum brightness temperature (not shown) found for oceanic systems does not simply reflect the presence of more mid-level (congestus) clouds over ocean as the results shown are specifically for large, deep systems (maximum $R > 300$ km, minimum $T_B < 220$ K).

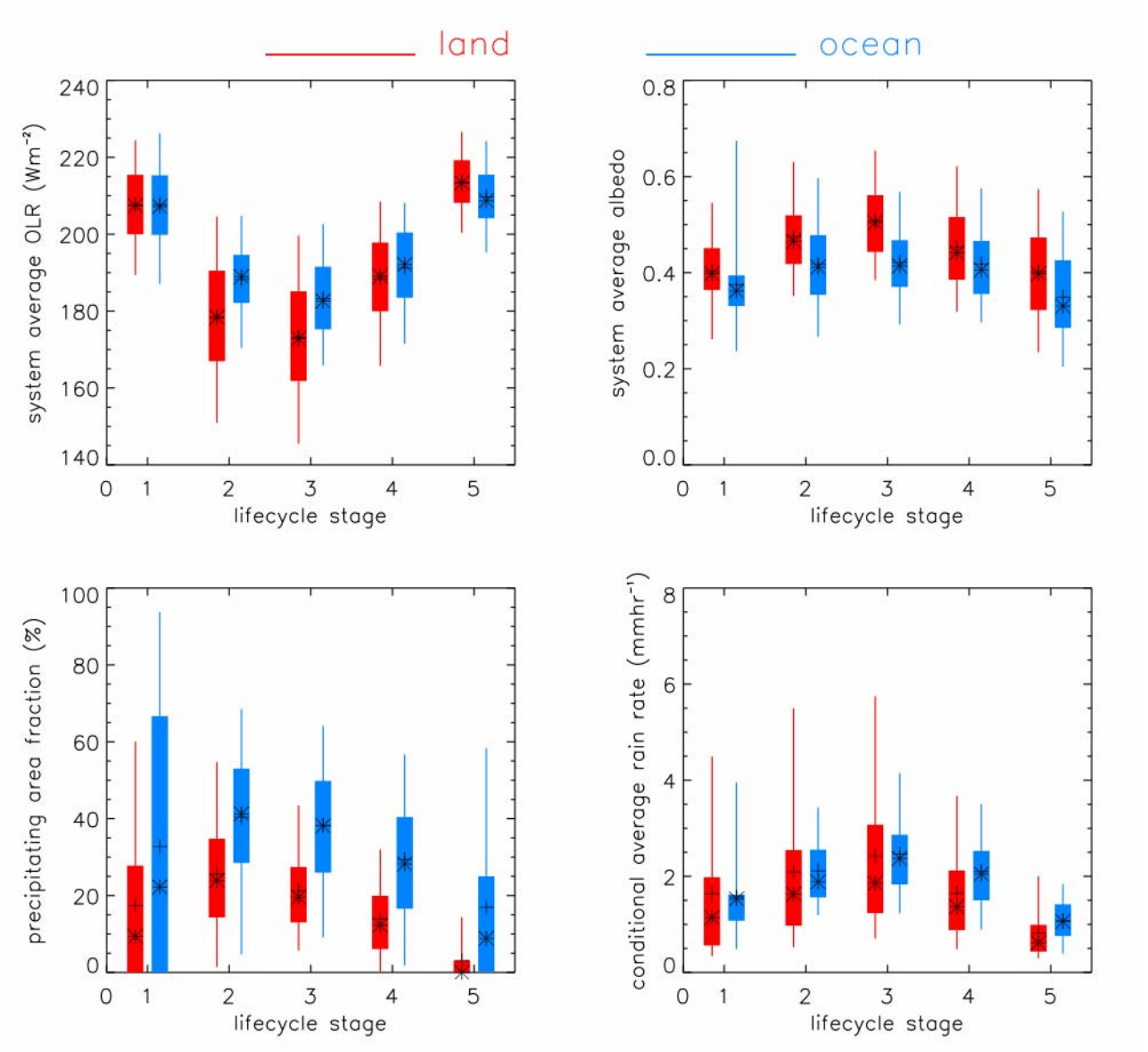

Figure 2. Comparison of the evolution of radiative (OLR, upper left and albedo upper right) and precipitation properties (precipitating area fraction, lower left and conditional average rain rate, lower right) for large deep Atlantic (ocean) and African (land) convective systems. The box covers 25-75th percentile and the whisker 5-95th. + indicates the mean and * the median value. Based on GERB-like and TRMM 3B42 data. Life-cycle stage numbers are defined in Figure 1.

Matched TRMM Precipitation Radar and Lightning Imager Data

The TRMM precipitation radar (PR) 2A23 dataset provides a classification of the observed rainfall as either convective or stratiform based on the vertical and horizontal structure of the radar echos (Awaka et al. 1997). Figure 3 shows the evolution of the convective and stratiform rain volume fractions for

both land and ocean systems. Over land, the expected evolution is observed, with convective rainfall dominating the developing and mature stages of the system evolution, and stratiform rain becoming more important as the systems dissipate. Over ocean, the lifecycle appears to be less well defined, with the stratiform rain fraction essentially constant throughout the life-cycle.

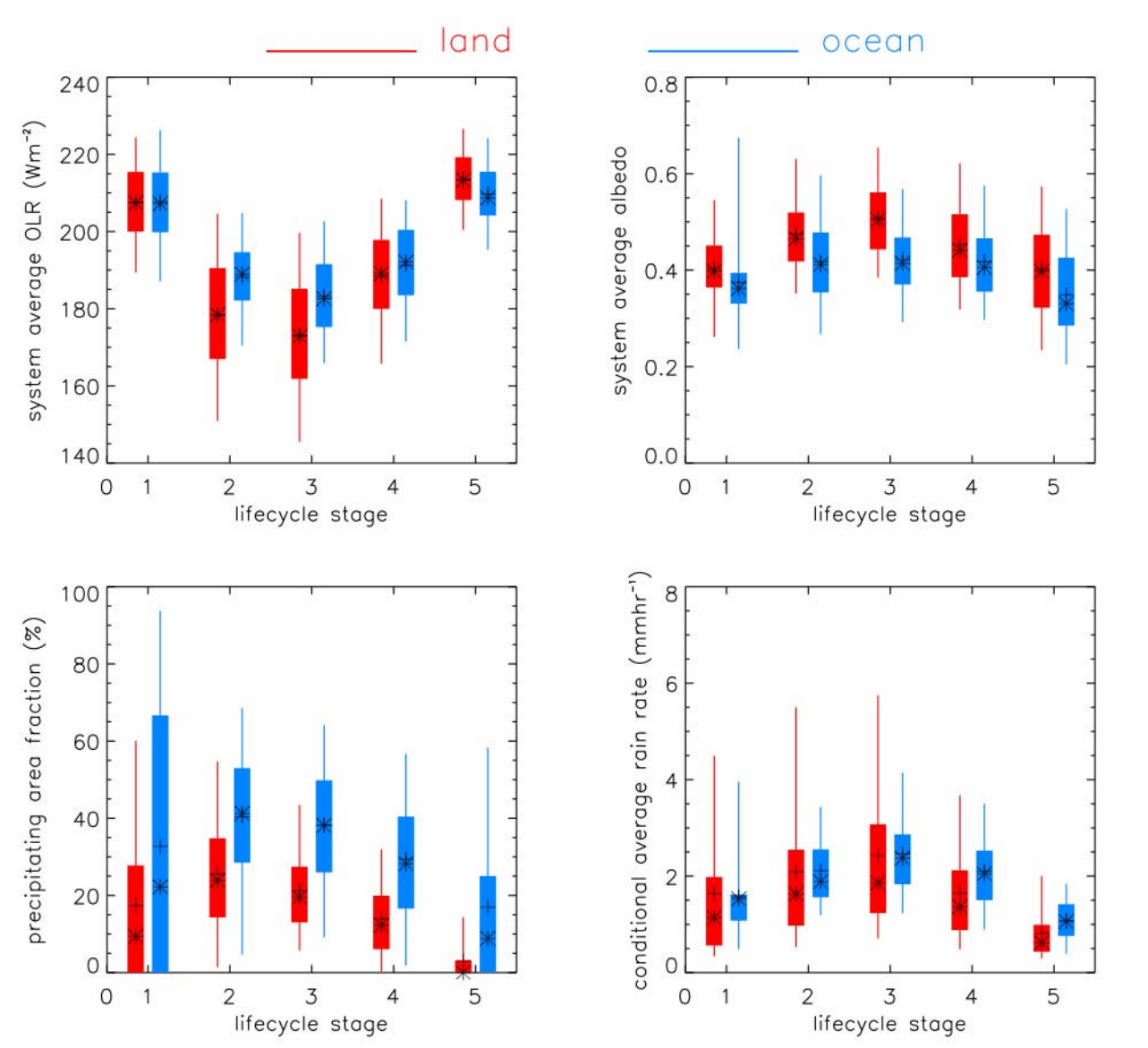

Figure 3. Convective and stratiform rain fractions (% of measured rain volume (rain rate x rain area) flagged as convective etc) as a function of life-cycle stage for large deep land and ocean convective systems. Life-cycle stage numbers are defined in Figure 1.

Differences in system evolution between land and ocean systems are also suggested in the plot of lightning occurrence shown in Figure 4. Lightning occurs where strong updrafts loft large particles into the mixed phase region (Zipser and Lutz 1994) and is therefore associated with active convection and heavy rainfall. Field campaign results suggest that updrafts are significantly weaker over ocean than over land, resulting in the much lower lightning frequency observed (e.g. Lucas et al. 1994).

Consistent with the PR data, lightning occurs most frequently in the convectively active developing and detraining stages over land. Over ocean, however, the peak occurs later in the lifecycle. Why this occurs is not clear, but may be related to the propagation of dissipating land based systems out over the coast of West Africa. Work is ongoing to investigate this further.

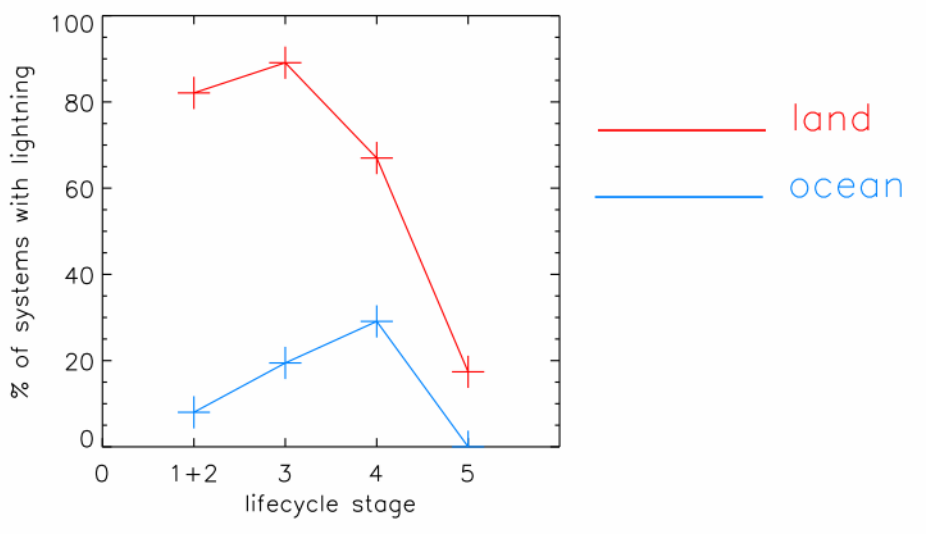

Figure 4. Lightning occurrence (% of sampled systems) as a function of life-cycle stage for large deep land and ocean systems. Life-cycle stage numbers are defined in Figure 1.

The ARM Mobile Facility at Niamey, Niger

The ARM mobile facility will be at Niamey in Niger during the convective season (JJAS) of 2006 as part of the AMMA field campaign, providing detailed, but localized measurements of passing storms. The framework described here will allow these data to be examined in the context of the wider population of African convective systems.

Figure 5 shows how systems passing over the site at Niamey during JJAS 2005 compare to the overall population of large, deep convective systems observed over Africa in this period. Storms passing over the site tend to be somewhat larger and deeper and more heavily precipitating than the average African storm.

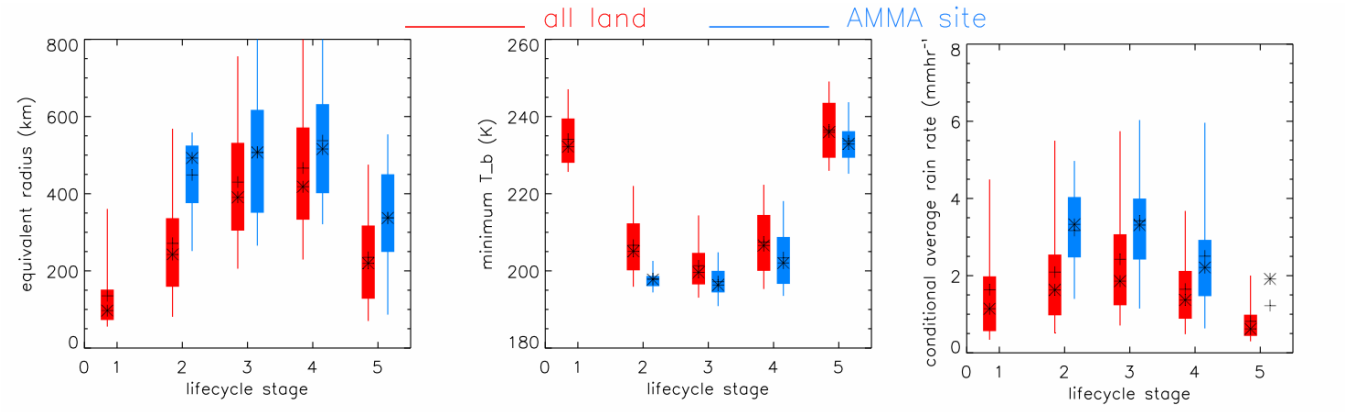

Figure 5. Comparison of system size (left), depth (center) and system average rain rate (right) for large deep systems passing over the ARM site at Niamey (AMMA site) with the overall African land population. Life-cycle stage numbers are defined in Figure 1.

To demonstrate the valuable information satellite data can provide as a context for more localized site based measurements, Figure 6 shows the temporal evolution of the system size and minimum brightness temperature, and Figure 7 shows the spatial structure of the OLR and rain-rate fields for a system sampled by PR as it passes over the ARM site. The system is observed close to its peak size, just as it begins to dissipate (decrease in R and increase in T). The PR sample occurs shortly after the core of the system has passed over the ARM site (marked as a cross in Figure 7), and provides good coverage of the system, sampling both the cold core and extended anvil region.

The radar reflectivity probability distribution for the region of the system sampled by PR is shown in Figure 8, together with the reflectivity profiles for the ARM site and two other example points. The high top of the distribution confirms the presence of deep precipitating clouds, and the presence of a clear bright band signal (spike at ~4.5 km altitude) indicates that the rainfall is primarily stratiform, as might be expected for a system in a mature to dissipating state.

No surface rainfall is detected by PR at the ARM site, despite signal aloft. Point A is typical of an active convective cell, while point B clearly shows a bright-band feature typical of stratiform rain. The decrease in reflectivity with height below the bright-band suggests evaporation of rain before reaching the surface in this part of the system.

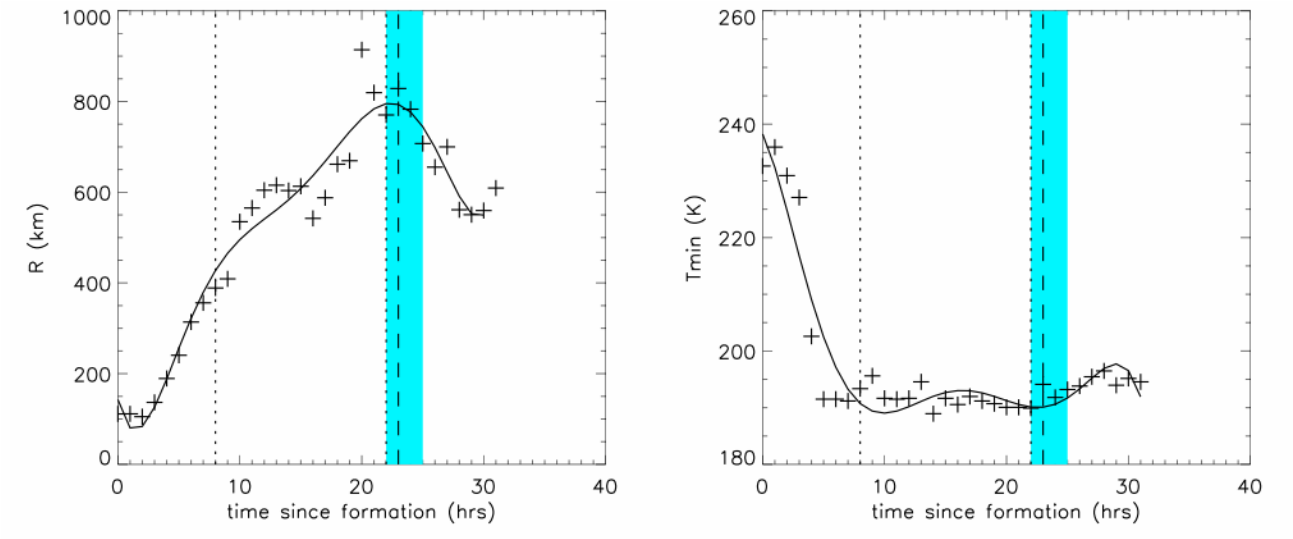

Figure 6. Evolution of system radius (left) and minimum brightness temperature (right) for a system passing over the ARM site at Niamey. Dotted vertical lines show the time when the minimum temperature is reached (end of developing stage), and the time of maximum radius (end of mature phase). The turquoise box indicates when the system passes over the ARM site, and the dashed line gives the time of the TRMM overpass.

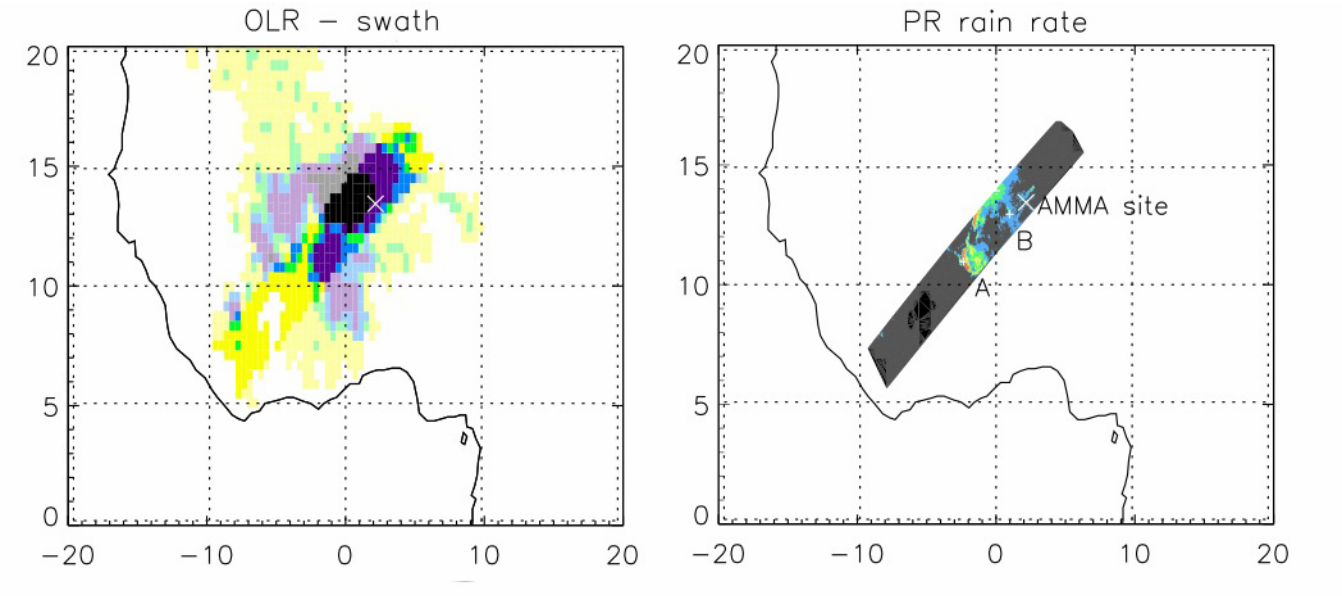

Figure 7. Spatial structure of the system shown in Figure 6 at the time of the TRMM overpass. The left panel shows the OLR for the entire system, with the region of the PR swath highlighted, and the right panel shows the PR observed rain rates. The location of the ARM site is marked with a cross in both panels. Points A and B indicate the locations of the reflectivity profiles shown in Figure 8.

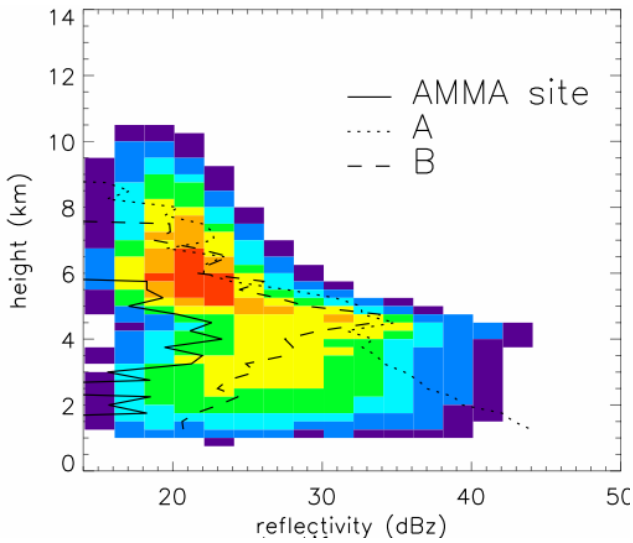

Figure 8. Probability distribution function of reflectivity by altitude for the portion of the system shown in Figures 6 and 7 sampled by the PR instrument. Profiles are also shown for the location of the ARM (AMMA) site, and for points A and B.

Summary

The evolution of system size and minimum brightness temperature for convective systems tracked using hourly thermal flux data is used to create a classification by life-cycle stage. This is shown to provide a valuable framework for the analysis of less well sampled datasets, allowing a composite picture of the evolution to be built up.

Convective systems over Africa are found to be deeper, with higher albedo and more frequent lightning than oceanic systems over the tropical Atlantic. A larger fraction of the cloud area is however found to be precipitating over the ocean.

As would be expected from the typical picture of convective system development, African systems peak in activity early in their development, with rainfall becoming more stratiform in nature as they evolve. In comparison, oceanic systems are have a less well defined life-cycle, remaining more active after the peak size is reached, with the peak in lightning activity occurring late in the lifecycle. This is postulated to be due to the propagation of dissipating continental systems out over the Atlantic region.

The deployment of the ARM Mobile Facility to Niamey, Niger, for the wet season of 2006 as part of the AMMA campaign will provide an excellent opportunity for detailed study of convective systems passing over the site. Here we show how satellite data, and the framework described here in particular, can be used to provide a context in which to interpret these valuable data. Systems passing over the site at Niamey tend to be observed relatively late in their development and are larger, deeper, and more heavily precipitating than the average large deep African storm.

Acknowledgements

TRMM PR data were obtained form the National Aeronautics and Space Administration Goddard DAAC, and LIS data were obtained from the Global Hydrology Resource Center. Nicolas Clerbaux at the Royal Meteorological Institute of Belgium kindly provided the GERB-like data.

Corresponding Author

JM Futyan, email: jfutyan@giss.nasa.gov, phone: +1 212 678 5592.

References

Awaka, J, T Iguchi, H Kumagai, and K. Okamoto. 1997. "Rain type classification algorithm for TRMM precipitation radar." In Proceedings 1997 International Geoscience and Remote Sensing Symposium, Singapore, IEEE, 1633-1635.

Boer, ER, and V Ramanathan. 1997. "Lagrangian approach for deriving cloud characteristics from satellite observations and its implication for cloud parameterization." *Journal of Geophysical Research* 102(D17).

Lucas, C, EJ Zipser, and MA LeMone. 1994. "Vertical velocity in oceanic convection off tropical Australia." *Journal of Atmospheric Science* 51:21.

Schumacher, C, and RA Houze, Jr. 2003. "Stratiform rain in the tropics as seen by the TRMM precipitation radar." *Journal of Climate* 16.

Zipser, EJ, and KR Lutz. 1994. "The vertical profile of radar reflectivity of convective cells: A strong indicator of storm intensity and lightning probability." *Monthly Weather Review* 122.